


# Numerical study of converting beat-note signals of dual-frequency lasers to optical frequency combs by optical injection locking of semiconductor lasers

Chenhao Liu(刘晨浩), Haoshu Jin(靳昊澍), Hui Liu(刘辉), and Jintao Bai(白晋涛)
**Citation:**Chin. Phys. B, 2022, 31 (**8**): 084205. DOI: 10.1088/1674-1056/ac649a
Journal homepage: http://cpb.iphy.ac.cn; http://iopscience.iop.org/cpb

**What follows is a list of articles you may be interested in**

---

## Precise determination of characteristic laser frequencies by an Er-doped fiber optical frequency comb

Shiying Cao(曹士英), Yi Han(韩羿), Yongjin Ding(丁永今), Baike Lin(林百科), and Zhanjun Fang(方占军)
Chin. Phys. B, 2022, 31 (**7**): 074207. DOI: 10.1088/1674-1056/ac5608

## All polarization-maintaining Er:fiber-based optical frequency comb for frequency comparison of optical clocks

Pan Zhang(张攀), Yan-Yan Zhang(张颜艳), Ming-Kun Li(李铭坤), Bing-Jie Rao(饶冰洁), Lu-Lu Yan(闫露露), Fa-Xi Chen(陈法喜), Xiao-Fei Zhang(张晓斐), Qun-Feng Chen(陈群峰), Hai-Feng Jiang(姜海峰)[‡], and Shou-Gang Zhang(张首刚)
Chin. Phys. B, 2022, 31 (**5**): 054210. DOI: 10.1088/1674-1056/ac40f6

## Interrogation of optical Ramsey spectrum and stability study of an $^{87}$Sr optical lattice clock

Jing-Jing Xia(夏京京), Xiao-Tong Lu(卢晓同), and Hong Chang(常宏)
Chin. Phys. B, 2022, 31 (**3**): 034209. DOI: 10.1088/1674-1056/ac11e0

## Eigenvalue spectrum analysis for temporal signals of Kerr optical frequency combs based on nonlinear Fourier transform

Jia Wang(王佳), Ai-Guo Sheng(盛爱国), Xin Huang(黄鑫), Rong-Yu Li(李荣玉), Guang-Qiang He(何广强)
Chin. Phys. B, 2020, 29 (**3**): 034207. DOI: 10.1088/1674-1056/ab683a

## Parallel generation of 31 tripartite entangled states based on optical frequency combs

Jing Zhang(张静), Yan-Fang Wang(王艳芳), Xiao-Yu Liu(刘晓宇), Rong-Guo Yang(杨荣国)
Chin. Phys. B, 2017, 26 (**12**): 124205. DOI: 10.1088/1674-1056/26/12/124205

---

# Numerical study of converting beat-note signals of dual-frequency lasers to optical frequency combs by optical injection locking of semiconductor lasers

Chenhao Liu(刘晨浩), Haoshu Jin(靳昊澍), Hui Liu(刘辉)†, and Jintao Bai(白晋涛)

*Institute of Photonics & Photon-technology, Northwest University, Xi'an* 710069, *China*

(Received 1 March 2022; revised manuscript received 30 March 2022; accepted manuscript online 6 April 2022)

The optical injection locking of semiconductor lasers to dual-frequency lasers is studied by numerical simulations. The beat-note signals can be effectively transformed to optical frequency combs due to the effective four wave-mixing in the active semiconductor gain medium. The low-noise Gaussian-like pulse can be obtained by locking the relaxation oscillation and compensating the gain asymmetry. The simulations suggest that pulse trains of width below 30 ps and repetition rate in GHz frequency can be generated simply by the optical injection locking of semiconductor lasers. Since the optical injection locking can broaden the spectrum and amplify the optical power simultaneously, it can be a good initial stage for generating optical frequency combs from dual-frequency lasers by multi-stage of spectral broadening in nonlinear waveguides.

**Keywords:** optical frequency combs, optical injection locking, dual-frequency lasers

**PACS:** 42.62.Eh, 42.60.Rn, 42.65.–k **DOI:** 10.1088/1674-1056/ac649a

## 1. Introduction

The optical frequency combs (OFCs) have broad applications,[1] including optical atomic clocks,[2–4] microwave photonics,[5] calibration of astronomical spectrographs,[6] LiDAR,[7] frequency comb spectroscopy,[8] and attosecond science.[9] From the view of frequency domain, OFCs are consist of a large number of modes with equidistant frequencies and fixed relative phase. Up to now, this kind of optical spectra can be implemented mainly by three technologies that is mode-locked laser,[10] electro–optic comb generator,[11,12] and microresonator.[13] Typically, these OFCs require cavity resonance to enhance optical oscillations, but the freedom of comb line spacing is largely limited. In fact, OFCs without optical cavity are possible, for example the electric–optic frequency comb based on the cascading of multi-modulators. However, the modulators may also impose some limitations, such as modulation bandwidth and the requirement for high-depth modulation.

An interesting proposal to generate OFC without optical resonator and modulator is to transform a dual-frequency beat signal into a train of pulse through the propagation in nonlinear optical fiber.[14–19] However, its development is hindered due to the requirements of high power for pumping, long path for spectral broadening, sophisticated dispersion management, and low-noise dual-frequency lasers, *etc*.

Fortunately, some technological advances are gradually breaking these restrains, making that proposal still quite attractive. To this end, the following investigation refers two interesting technologies. The first one is the the low-noise dual-frequency laser (DF-laser) that can be achieved by sustaining two lasers in a common cavity. Such kind of dual-frequency lasers can be realized in platforms of VECSEL,[20–25] solid-state laser,[26,27] fiber lasers,[28,29] *etc*. By this device, low-noise optically carried radio frequency (RF) can be generated even in free running due to the elimination of the common noises. This dual-frequency is equivalent to singe side-band modulation but with a high modulation depth which is closing to one. Moreover, the optically carried RF can be broadly tuned without the limitation of modulation bandwidth. The second one is the multimode optical injection locking (OIL) which can be an effective way of wave-mixing. It has been demonstrated that optical injection of OFC into semiconductor lasers can broaden the spectrum effectively due to the strong four wave-mixing.[30,31]

This paper reports an investigation of the possibility to generate an OFC by optical injection locking a semiconductor laser to a DF-laser by numerical simulations. In addition to the process of dual-frequency optical injection, the simulations also consider the random noises from spontaneous emissions. The evolution of output power, carrier number, and optical phase are simulated, from which the spectra, and phase/intensity noises can be derived. The pulse width of the OFC generated with this way can be less than 30 ps. Moreover, the pulse shape can be controlled to be Gaussion-like. Comparing to the way of sending the DF-laser to high nonlinear fiber directly, optical injection allows to start from low power, or to reduce the length of nonlinear fiber thereby alleviate the suffering from dispersion induced phase mismatching. We thus expect it can offer a good initial stage of OFCs generation with DF-laser, whose spectra can be further broadened

†Corresponding author. E-mail: liuhui_gzs@nwu.edu.cn

© 2022 Chinese Physical Society and IOP Publishing Ltd 

in nonlinear waveguides, giving a broadband OFC without external modulation and can be agile in central wavelength and comb spacing.

## 2. The model of dual-frequency laser optical injection

Supposing the slave laser is a distributed feedback (DFB) semiconductor laser, we model the dynamics of carrier number $N(t)$, number of photons inside the cavity $S(t)$, and optical phase $\Theta(t)$ by the rate equations as following:

$$\frac{\mathrm{d}N(t)}{\mathrm{d}t} = \frac{I(t)}{e} - \frac{N(t)}{\tau_\mathrm{n}} - g\frac{N(t)-N_0}{1+\varepsilon S(t)}S(t) + F_N(t), \tag{1}$$

$$\frac{\mathrm{d}S(t)}{\mathrm{d}t} = g\frac{N(t)-N_0}{1+\varepsilon S(t)}S(t) - \frac{S(t)}{\tau_\mathrm{p}} + \frac{\beta N(t)}{\tau_\mathrm{n}} + F_S(t) + \frac{2K}{\tau_\mathrm{in}}\sqrt{S_0 S(t)}\sum_{q=Q_1}^{Q_2} C_q \cos\left[q\omega_r t + \Delta\omega t - \Theta(t)\right], \tag{2}$$

$$\frac{\mathrm{d}\Theta(t)}{\mathrm{d}t} = \frac{\alpha}{2}g\left[N(t)-\overline{N}\,\right] + F_\Theta(t) + \frac{K}{\tau_\mathrm{in}}\sqrt{\frac{S_0}{S(t)}}\sum_{q=Q_1}^{Q_2} C_q \sin\left[q\omega_r t + \Delta\omega t - \Theta(t)\right], \tag{3}$$

where $I(t)$ is the injected current of the DFB laser, $e$ is the electron charge, $\tau_\mathrm{n}$ is the carrier lifetime, $g$ is the gain coefficient, $\tau_\mathrm{p}$ is the photon lifetime, $N_0$ is the carrier number at transparency, $\overline{N}$ is the time-averaged carrier number, $\beta$ is the fraction of spontaneous emissions fallen into the lasing mode, $\alpha$ the Henry's factor, $\varepsilon$ the nonlinear gain compression factor. Langevin terms $F_i(t)$ $(i = N, S, \Theta)$ express the laser noises originating from the spontaneous emissions. Although only the DF-laser optical injection is considered, the comb spectral laser injection expressed by the terms in summation notation in Eqs. (2) and (3) is introduced here to generalize the model to the optical injection of OFC. Here, $K$ defines the ratio of the amplitude of the injected light field to the amplitude of the output light field in steady-state without the injected light field, $\tau_\mathrm{in}$ the round-trip time of photon inside the DFB laser cavity, $C_q$ the coefficient of the $q$-th comb mode, $Q_1$ and $Q_2$ the starting number and ending number of the comb modes, $\omega_r$ the angular frequency of the mode spacing of OFC, $\Delta\omega$ the detuning of the free running slave laser to the nearest comb mode. The current injected into the DFB laser can be conveniently quantified by the current threshold value, *i.e.*,

$$I(t) = rI_\mathrm{th} = r\frac{e}{\tau_\mathrm{n}}\left(N_0 + \frac{1}{g\tau_\mathrm{p}}\right).$$

For simplicity, we suppose an OFC with flattened spectrum is used, meaning $C_q \equiv 1$. The output optical power $P(t)$ can be derived by $P(t) = \eta_\mathrm{d}(h\nu/\tau_\mathrm{p})S(t)$, where $\eta_\mathrm{d}$ is the differential quantum efficiency, $h$ the Planck's constant. By solving the coupled equations without the Langevin terms and optical injection terms, $S_0$ and $\overline{N}$ are obtained by

$$\overline{N} = \frac{\tau_\mathrm{n}}{e}\frac{I(1+\varepsilon S) + gN_0 eS}{1+\varepsilon+gS\tau_\mathrm{n}}$$

with $a = e(\varepsilon + g\tau_\mathrm{n})$, $b = e + g\tau_\mathrm{p}[(1-\beta)N_0 e - \tau_\mathrm{n} I] - \beta\varepsilon\tau_\mathrm{p} I$, $c = \beta\tau_\mathrm{p} I$, where $I$ is the injection current at steady-state. The Langevin terms can be simulated with three Gaussian random variables whose self- and crossed-correlations can be generally expressed as $\langle F_i(t)\rangle = 0$, $\langle F_i(t)F_j(t)\rangle = 2D_{ij}\delta(t-t')$, where $\delta(t-t')$ is Dirac's delta function and $D_{ij}$ is the diffusion coefficient defined as $2D_{SS}(t) = 2\beta N(t)S(t)/\tau_\mathrm{n}$, $2D_{NN}(t) = (2N(t)/\tau_\mathrm{n})[1+\beta S(t)]$, $2D_{\Theta\Theta}(t) = \beta N(t)/2\tau_\mathrm{n}S(t)$, $2D_{SN}(t) = -2\beta N(t)S(t)/\tau_\mathrm{n}$, $2D_{S\Theta}(t) = 0$, $2D_{N\Theta}(t) = 0$. These cross-correlated Langevin terms can be generated with three independent white Gaussian random variables $x_S$, $x_\Theta$, and $x_Z$ as follows:[32]

$$F_S(t) = \sqrt{\frac{2D_{SS}(t)}{\Delta t}}x_S, \tag{4}$$

$$F_\Theta(t) = \sqrt{\frac{2D_{\Theta\Theta}(t)}{\Delta t}}x_\Theta, \tag{5}$$

$$F_Z(t) = \sqrt{\frac{2D_{ZZ}(t)}{\Delta t}}x_Z, \tag{6}$$

$$F_N(t) = F_Z(t) - F_S(t) \tag{7}$$

with $2D_{ZZ} = 2N(t)/\tau_\mathrm{n}$.

## 3. The simulation results and discussion

To help in understanding the dynamics, the optical injection of dual-frequency laser is compared to the instances of single-frequency laser (SF-laser) injection, and free-running, as shown together in Fig. 1 to indicate the difference. The spectra in Fig. 1(a) show that two peaks are sided around the optical carrier when a SF-laser is injected, whereas the random noises are substantially suppressed comparing to the free-running laser. The two side peaks indicate the strong relaxation oscillation under the high seeding power OIL. We call these peaks as relaxation oscillation peak (RO-peak). In fact, injected light-induced pulsations (ILIP) may happen according to the well-known theory of SF-laser injection.[33] With the knowledge of this phenomenon, the beat-note frequency of the injected DF-laser is chosen to coincide the RO-peak, leading to an efficient generation of new tones. These new tones are the results of four wave-mixing (FWM) effect in semiconductor lasers, which has been explained by the light induced gain grating and index grating.[34] Figure 1(a) shows that there are 10 tones above the random noises after the DF-laser injected with a seeding power of $K = 10^{-5/20}$. The reason why the efficient FWM happens can be explained by Fig. 1(b) which shows the carrier population pulsation and the pulsed modulation of optical phase, corresponding the dynamic gain grating and index grating. To distinguish it from SF-laser ILIP,

we call it DF-laser ILIP. Moreover, the tones are symmetrically distributed around the optical carrier. This symmetry is obtained by the balance between two asymmetries. One comes from the asymmetry injection of the DF-laser, since one component of the injected light is used for locking the slave laser, the other component is right sided, as indicated by the arrows in Fig. 1(a). The other asymmetry comes from the gain asymmetry introduced by Henry's factor, which leads to the higher gain at lower (left) frequencies. Thanks to this symmetry spectrum, the generated pulse is Gaussian-like, as shown in Fig. 1(b). Figures 1(c)–1(d) show the power spectral density of the phase and intensity, which illustrates that the random noises around the RO-peak are greatly suppressed and replaced by a new tone. It means that the RO-peak is locked to the beat-note frequency and gives a low-noise pulse train. This is a big difference between the DF-laser ILIP and SF-laser ILIP. However, except the region nearby the RO-peak, random noises in DF-laser injection are more than that of SF-laser injection, which can be attributed to the interference between the comb lines.

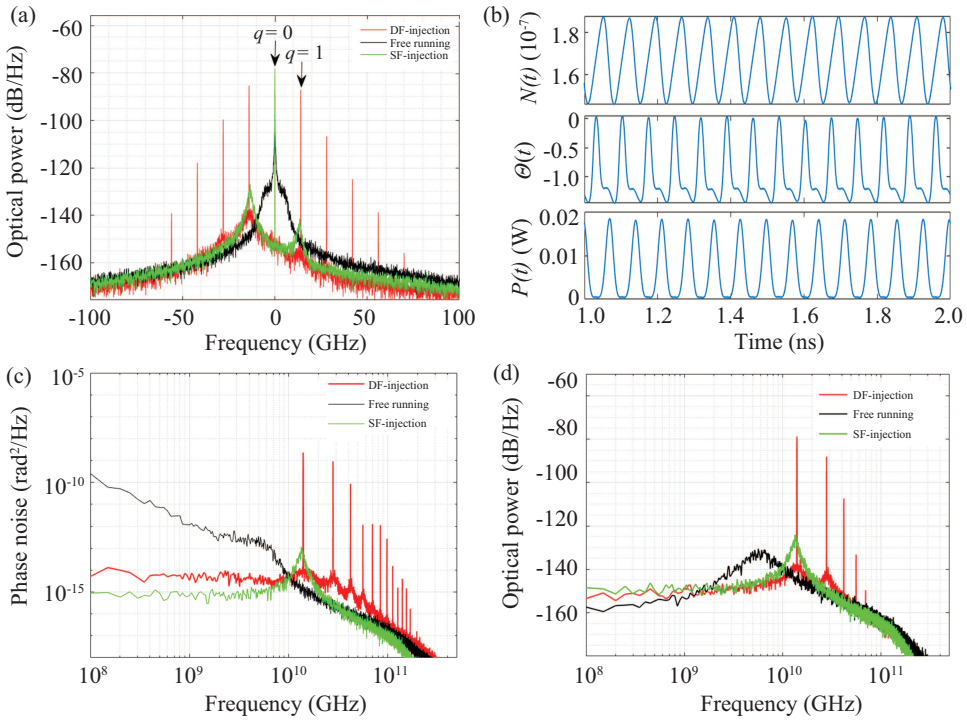



**Fig. 1.** A simulation of dual-frequency injection (DF-injection) to a single-mode semiconductor laser: (a) the spectra; (b) the evolution of carrier number $N(t)$, output power $P(t)$, and the optical phase $\Theta(t)$; (c) the power spectral densities of the phase noises; (d) the power spectral densities of RINs. The circumstances of free running and single-frequency injection (SF-injection) are shown together. The parameters used in this simulation are listed in Table 1.

**Table 1.** Parameters used in the simulations for Fig. 1.

| Symbol | Definition | Value |
|---|---|---|
| $r$ | ratio of current injected to DFB laser to its threshold value | 3 |
| $\Delta t$ (ps) | time interval for integration of the differential equations | 1 |
| $\tau_{\rm in}$ (ps) | round-trip time of photon inside the DFB laser cavity | 6 |
| $\tau_{\rm n}$ (ns) | lifetime of the carriers | 0.33 |
| $\tau_{\rm p}$ (ps) | lifetime of photon inside the DFB laser cavity | 7.15 |
| $g$ ($\rm s^{-1}$) | gain slope coefficient | $1.13\times10^{4}$ |
| $\varepsilon$ | nonlinear gain compression factor | $4.58\times10^{-8}$ |
| $\beta$ | proportion of the spontaneous emissions fallen into the lasing mode | $3.54\times10^{-5}$ |
| $N_0$ | carrier number at transparency | $8.2\times10^{6}$ |
| $Q_1$ | starting number of the injected OFC modes | 0 |
| $Q_2$ | ending number of the injected OFC modes | 1 |
| $\eta_{\rm d}$ | differential quantum efficiency | 0.21 |
| $K$ | ratio of the amplitude of the injected light field to the amplitude of the output light field in steady-state without the injected light field | $10^{-5/20}$ |
| $\alpha$ | linewidth enhancement factor | 3 |
| $\omega_{\rm beat}=\omega_r$ (rad/s) | angular frequency of mode spacing of the OFC | $2\pi\times14\times10^{9}$ |
| $I_{\rm th}$ (mA) | threshold current value, $I_{\rm th}=(1.69\times10^{-19}/\tau_{\rm n})(N_0+1/g\tau_{\rm p})$ | 9.0 |

The above simulations raise a question that whether it is necessary to lock the RO-peak. To investigate this problem, the beat-note frequency is tuned from 2 GHz to 14 GHz, as shown in Fig. 2. When the beat-note frequency is well below RO-peak frequency, lots of tones are generated and the RO-peaks are overwhelmed by the new tones. However, RO is embedded in each pulse waveform, so that the pulses are severely deformed to be away from Gaussian-like. As the beat-note frequency is close to RO-peak frequency, the pulse form becomes more Gaussian-like, giving a higher peak power. However, when beat-note frequency is well above RO-peak frequency, the RO-peaks are set to be free, giving some random noises and reducing the efficiency of the FWM. Therefore, choosing the beat-note frequency closing to RO-peak frequency is important for the efficiency of FWM and the random noise suppression.

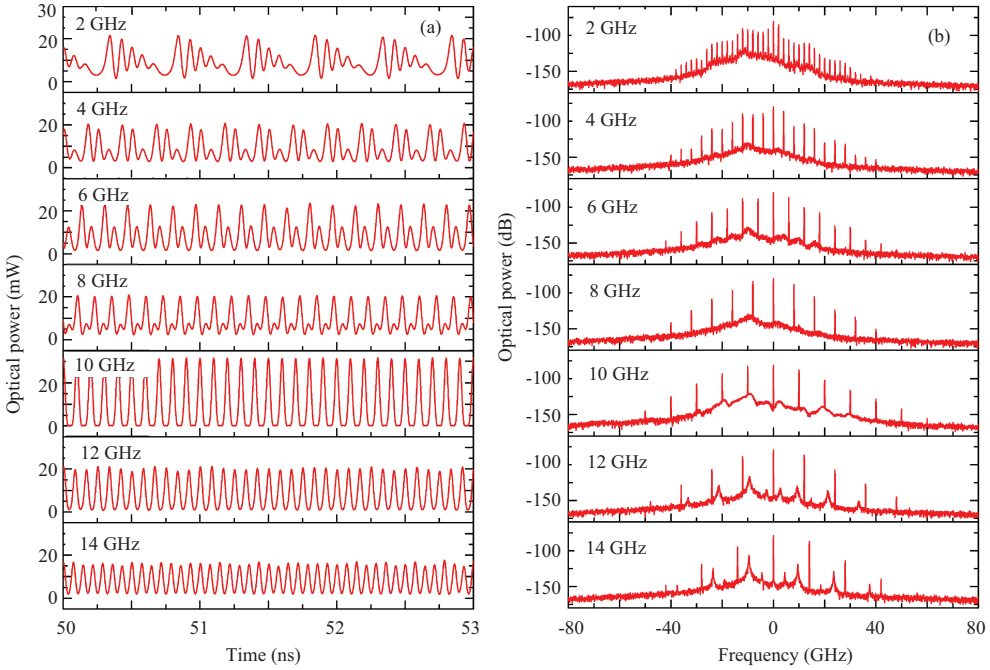



**Fig. 2.** The dependence of pulse shape and spectra on the beat-note frequency of the injected DF-laser: (a) the output pulse train, (b) the spectra. In these simulations, the value of seeding power is $K = 10^{-10/20}$. The parameters not indicated here are the same as those used in the simulation of Fig. 1.

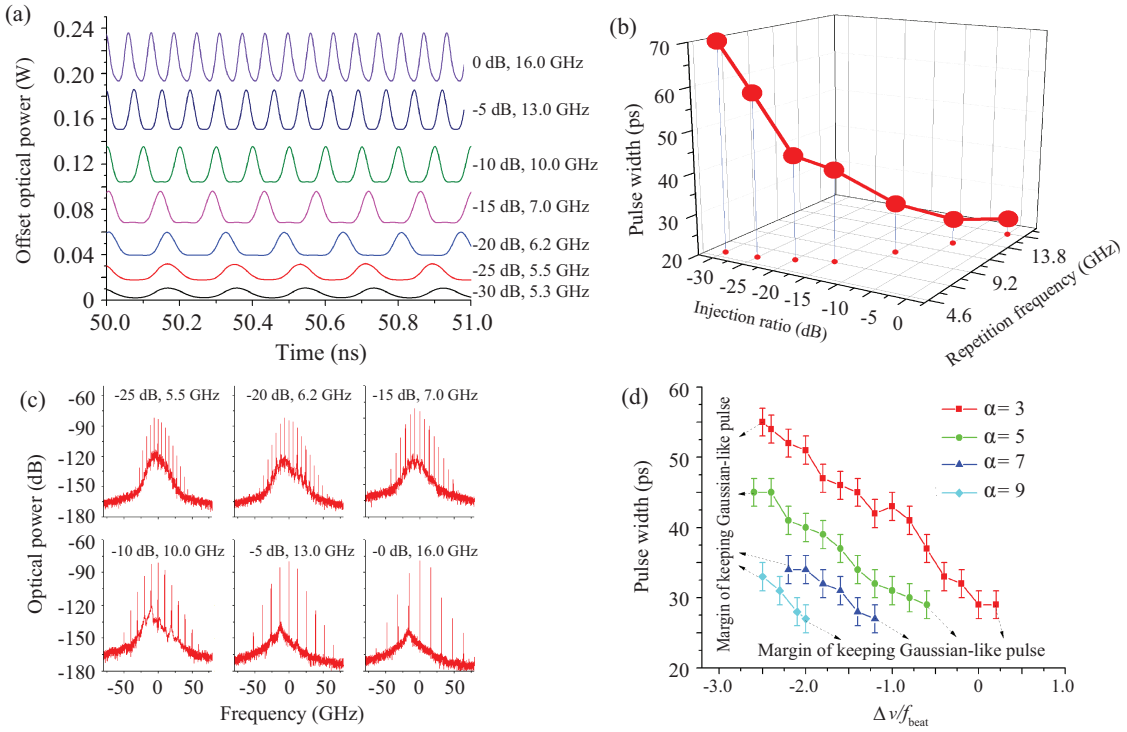



**Fig. 3.** The simulations with Gaussian-like pulse output: (a) the pulse train, (b) the pulse width, (c) spectra at different combination of seeding power and beat-note frequency, (d) the dependence of the pulse width of Gaussian-like output on the value of Henry's factor $\alpha$. The injection ratio in unit dB is equal to $20\log_{10}(K)$. $\Delta\nu$ denotes the free running slave laser frequency detuned from the master laser frequency of $q = Q_1 = 0$, $f_{\text{beat}}$ is the beat-note frequency. The parameters not indicated here are the same as those used in the simulation of Fig. 1.

It seems that beat-note frequency is constrained by the RO-peak frequency. This constrain can be lifted by the freedom of varying the seeding power. Figure 3(a) shows an example where Gaussian-like pulse output can be achieved in the repetition frequency range from 5.3 GHz to 16.0 GHz by varying the seed power. The corresponding pulse widths are plotted in Fig. 3(b), showing that not only the repetition rate becomes higher, but also the pulse becomes shorter. Pulses as short as below 30-ps is possible. Additionally, higher seeding power can also suppress the random noises in a higher degree, as shown in Fig. 3(c). However, when the repetition rate frequency goes higher, the tones become fewer, which is limited by the bandwidth of single longitudinal mode. As a result, the pulse width is limited to be about 30 ps. Generally, it is desirable to use the lowest possible seeding power to generate optical frequency combs with the lowest possible noise. Given these requirements, the 10-GHz is a value approaching the optimum beat-note frequency, where the seeding power is only about $-10$ dB, and the width of Gaussian-like pulse can reach the 30-ps limitation. Additionally, the value of $r$ is another variable to change the RO-peak frequency, but its effect is small as will be shown in Fig. 4. In principle, the values of $\tau_p$ and $\tau_n$ can also be used to change the RO-peak frequency, but they are not controllable for a given DFB semiconductor laser. Although these two intrinsic parameters are engineerable, the typical values are more practical for experiments.

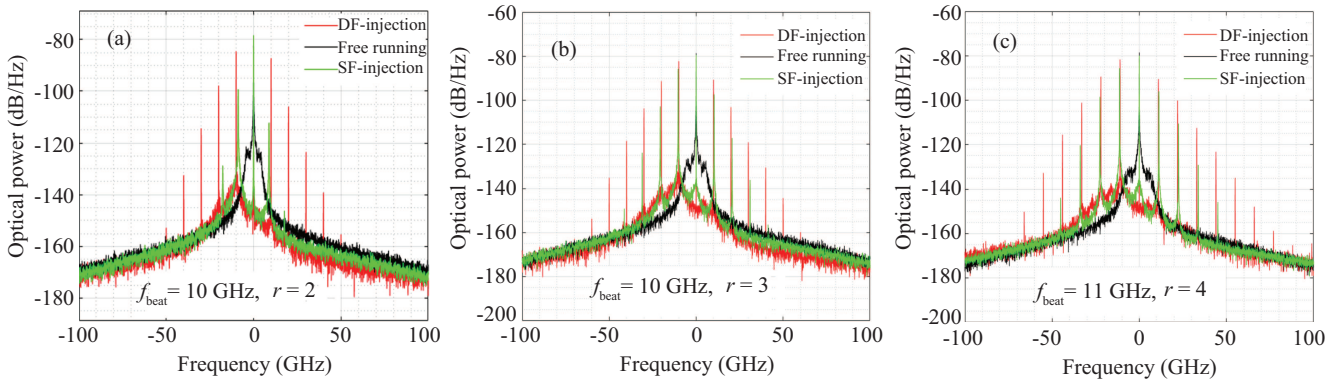



**Fig. 4.** Enhancement of the ILIP by increasing the excitation ratio $r$. Panels (a)–(c) show the spectra of the simulation with $r = 2$, 3, and 4, respectively. The corresponding pulse width is 36 ps, 30 ps, and 27 ps, respectively. The parameters not indicated here are the same as those used in the simulation of Fig. 1.

Another import aspect for OIL is the detuning. Figure 3(d) shows that the Gaussian-like pulse form can be kept in the detuning range of $\Delta\nu/f_{beat} = -2.5$ to $\Delta\nu/f_{beat} = 0.2$ when $\alpha = 3$, where $\Delta\nu$ denotes the free running slave laser frequency detuned from the master laser frequency of $q = Q_1 = 0$, $f_{beat}$ is the beat-note frequency. It suggests that the working region is shifted to the negative detuning where the gain is higher due to the amplitude/phase coupling effect. Therefore, as the value of $\alpha$ increases, the preference for negative detuning becomes more, but the working range for Gaussian-like pulse output becomes smaller. However, the detuning towards positive can give shorter pulses because the lower gain at higher optical frequency can be compensated by the injected field, leading to a broader spectrum.

Since RO can help to build shorter pulse, it makes sense to investigate the OIL under stronger RO. Figure 4 shows the results when the carrier excitation ratio $r$ changes. One can see that stronger RO-peak can be built with higher value of $r$. If the $r$ value is high enough, some comb-like tones can be built even with SF-laser injection, which indicates the happening of SF-laser ILIP. When the DF-laser is injected into, the RO is locked to the injected light and builds shorter pulses.

## 4. Conclusion

In conclusion, the optical injection locking of single-mode semiconductor lasers to DF-lasers is studied by numerical simulation. This optical injection can generate an OFC due to the efficient FWM effect created by the nonlinear gain medium inside the semiconductor laser. Choosing the beat-note frequency of the DF-laser closing to RO-peak is very important for generating Gaussian-like pulses. Moreover, the RO can be locked to the beat-note frequency of the DF-laser, thus can suppress the random noise greatly. The RO-peak frequency can be tuned by changing the seeding power. Therefore, the repetition rate of the Gaussian-like pulse can also be tuned this way. Low repetition rate gives more random noise, but higher frequency creates less new tones. Gaussian-like pulse shape can be kept within a certain range of detuning, and this detuning tend to be negative due to the gain symmetry. However, the shortest pulse happens at the margin towards to positive. Additionally, stronger RO can be helpful to build shorter pulses, which can be realized by increasing the carrier excitation ratio. The RO-peak frequency can be tuned by the controllable variables, such as seeding power, and carrier excitation ratio, but also governed by the intrinsic parameters, including carrier lifetime, and photon lifetime inside the cavity. For the semiconductor laser exampled here, the beat-

note frequency about 10 GHz is a value closing to the optimum, which can reach the pulse width below 30 ps. Although the pulse width cannot go down to femtosecond directly, this OFC can be furtherly broadened by nonlinear waveguides, for example the silicon-nitride waveguide.[35] Since there is no need of complex modulation or high-Q cavity, DF-laser optical injection can be a good option for realizing a simple, compact, low-cost, and robust OFC with a repetition rate around 10 GHz. This kind of OFC can be widely used in optical arbitrary waveform generation, microwave photonics, and optical coherent communication applications.[12]

## Acknowledgment

Project supported by the National Natural Science Foundation of China (Grant No. 62005215).

## References

[1] Diddams S A, Vahala K and Udem T 2020 *Science* **369**
[2] Nicholson T L, Campbell S L, Hutson R B, Marti G E, Bloom B J, McNally R L, Zhang W, Barrett M D, Safronova M S, Strouse G F, Tew W L and Ye J 2015 *Nat. Commun.* **6** 6896
[3] Kong D H, Wang Z H, Guo F, Zhang Q, Lu X T, Wang Y B and Chang H 2020 *Chin. Phys. B* **29** 070602
[4] Lin Y G and Fang Z J 2018 *Acta Phys. Sin.* **67** 160604 (in Chinese)
[5] Lucas E, Brochard P, Bouchand R, Schilt S, Sudmeyer T and Kippenberg T J 2020 *Nat. Commun.* **11** 374
[6] Steinmetz T, Wilken T, Araujo-Hauck C, Holzwarth R, Hansch T W, Pasquini L, Manescau A, D'Odorico S, Murphy M T, Kentischer T, Schmidt W and Udem T 2008 *Science* **321** 1335
[7] Ghelfi P, Laghezza F, Scotti F, Serafino G, Capria A, Pinna S, Onori D, Porzi C, Scaffardi M, Malacarne A, Vercesi V, Lazzeri E, Berizzi F and Bogoni A *Nature* **507** 341
[8] Picqué N and Hnsch T W 2019 *Nat. Photon.* **13** 146
[9] Corkum P B and Krausz F 2007 *Nat. Phys.* **3** 381
[10] Cundiff S T, Ye J and Hall J L 2001 *Rev. Sci. Instrum.* **72** 3749
[11] Parriaux A, Hammani K and Millot G 2020 *Adv. Opt. Photon.* **12** 223
[12] Torres-Company V and Weiner A M 2014 *Laser Photon. Rev.* **8** 368
[13] Kippenberg T J, Holzwarth R and Diddams S A 2011 *Science* **332** 555
[14] Chernikov S V, Dianov E M, Richardson D J, Laming R I and Payne D N 1993 *Appl. Phys. Lett.* **63** 293
[15] Tong Z, Wiberg A O, Myslivets E, Kuo B P, Alic N and Radic S 2012 *Opt. Express* **20** 17610
[16] Myslivets E, Kuo B P, Alic N and Radic S 2012 *Opt. Express* **20** 3331
[17] Antikainen A and Agrawal G P 2015 *J. Opt. Soc. Am. B* **32** 1705
[18] Antikainen A and Agrawal G P 2018 *J. Opt. Soc. Am. B* **35** 1733
[19] Slavik R, Parmigiani F, Gruner-Nielsen L, Jakobsen D, Herstrom S, Petropoulos P and Richardson D J 2011 *IEEE Photon. Technol. Lett.* **23** 540
[20] Scheller M, Baker C W, Koch S W, Moloney J V and Jason Jones R 2017 *IEEE Photon. Technol. Lett.* **29** 790
[21] Baili G, Morvan L, Alouini M, Dolfi D, Bretenaker F, Sagnes I and Garnache A 2009 *Opt. Lett.* **34** 3421
[22] Liu H, Gredat G, De S, Fsaifes I, Ly A, Vatre R, Baili G, Bouchoule S, Goldfarb F and Bretenaker F 2018 *Opt. Lett.* **43** 1794
[23] Liu H, Gredat G, Baili G, Gutty F, Goldfarb F, Sagnes I and Bretenaker F 2018 *J. Light. Technol.* **36** 3882
[24] Gredat G, Chatterjee D, Baili G, Gutty F, Sagnes I, Goldfarb F, Bretenaker F and Liu H 2018 *Opt. Express* **26** 26217
[25] Zhang P, Mao L, Zhang X, Wang T, Wang L and Zhu R 2021 *Opt. Express* **29** 16572
[26] Pillet G, Morvan L, Brunel M, Bretenaker F, Dolfi D, Vallet M, Huignard J-P and Le Floch A 2008 *J. Light Technol.* **26** 2764
[27] Hu M, Ke Y, Li Q, Zhou X, Lu Y, Yang G and Bi M 2019 *Opt. Express* **27** 13773
[28] Tan Y N, Jin L, Cheng L, Quan Z, Li M and Guan B O 2012 *Opt. Express* **20** 6961
[29] Ducournau G, Szriftgiser P, Akalin T, Beck A, Bacquet D, Peytavit E and Lampin J F 2011 *Opt. Lett.* **36** 2044
[30] Doumbia Y, Malica T, Wolfersberger D, Panajotov K and Sciamanna M 2020 *Opt. Lett.* **45** 435
[31] Doumbia Y, Malica T, Wolfersberger D, Panajotov K and Sciamanna M 2020 *Opt. Express* **28** 30379
[32] Fatadin I, Ives D and Wicks M 2006 *IEEE J. Quantum Electron.* **42** 934
[33] Mogensen F, Olesen H and Jacobsen G 1985 *IEEE J. Quantum Electron.* **21** 784
[34] Agrawal G P 1988 *J. Opt. Soc. Am. B* **5** 147
[35] Carlson D R, Hickstein D D, Zhang W, Metcalf A J, Quinlan F, Diddams S A and Papp S B 2018 *Science* **361** 1358